

See discussions, stats, and author profiles for this publication at: <https://www.researchgate.net/publication/26333476>

Fixation of the Two Tabun Isomers in Acetylcholinesterase: A QM/MM Study

ARTICLE *in* THE JOURNAL OF PHYSICAL CHEMISTRY B · AUGUST 2009

Impact Factor: 3.3 · DOI: 10.1021/jp903843s · Source: PubMed

CITATIONS

21

READS

37

4 AUTHORS, INCLUDING:



Max Malacria

Pierre and Marie Curie University - Paris 6

465 PUBLICATIONS 10,695 CITATIONS

[SEE PROFILE](#)



Etienne Derat

Pierre and Marie Curie University - Paris 6

64 PUBLICATIONS 1,234 CITATIONS

[SEE PROFILE](#)

Fixation of the Two Tabun Isomers in Acetylcholinesterase: A QM/MM Study

Ophélie Kwasnieski,[†] Laurent Verdier,[‡] Max Malacria,[†] and Etienne Derat^{*,†}

Institut de chimie moléculaire (UMR CNRS 7201), UPMC Univ Paris 06, C. 229, 4 place Jussieu, 75005 Paris, France, and Division Risque-Simulation-Caractérisation, Centre d'Etudes du Bouchet, BP n°3, 91710 Vert le Petit, France

Received: April 27, 2009; Revised Manuscript Received: June 10, 2009

Dysfunction of acetylcholinesterase (AChE) due to inhibition by organophosphorus (OP) compounds is a major threat since AChE is a key enzyme in neurotransmission. To more rigorously design reactivation agents, it is of prime importance to understand the mechanism of inhibition of AChE by OP compounds. Tabun is one of the more potent nerve agents. It is produced as a mixture of two enantiomers, one of them (the levorotatory isomer) being 6.3 times more potent. Could it be that the inhibition mechanism is different for the two enantiomers? To address this critical issue, we used a hybrid quantum mechanics/molecular mechanics (QM/MM) methodology. Calculations were performed using BP86 functional and TZVP basis set. Single points were also done with B3LYP and PBE0 functionals. We studied the four possible attacks of tabun on the oxygen of Ser203 using two crystallographic structures (PDB codes 2C0P and 3DL7): (*S*) tabun with the cyano group *syn* to the oxygen of Ser203 and (*R*) tabun with the cyano group *anti*, corresponding to the experimental X-ray structure; (*S*) tabun with the cyano group *anti* to the oxygen of Ser203 and (*R*) tabun with the cyano group *syn*, leading to a different isomer than was experimentally seen. We found that the most active enantiomer is (*S*) tabun with the cyano group *syn* to the oxygen of Ser203. Thus it seems that the cyano group does not leave *anti* to the oxygen of Ser203 due to repulsive polar interactions between cyanide and aromatic residues in the active site.

Introduction

Acetylcholinesterase (AChE) is a key enzyme in neurotransmission. It is one of the most efficient enzymes as its turnover rate is about 10^4 s⁻¹. AChE catalyzes hydrolysis of acetylcholine in choline and acetic acid and thus regenerates cholinergic neuron.^{1–3} The catalytic site is inside a gorge of about 20 Å. As seen in Scheme 1, the catalytic cycle involves a catalytic triad composed of Ser203, His447, and Glu334 in mouse AChE. The oxyanion hole composed of Ala204, Glu121, and Glu122 is very important as it activates the substrate via hydrogen bonds,^{4,5} as previously shown theoretically by Warshel et al.⁶ The acylation reaction of AChE by acetylcholine was modeled by McCammon et al. using a hybrid quantum mechanics/molecular mechanics (QM/MM) approach. It clarifies the role of the catalytic triad, in particular Glu334, and of the oxyanion hole.⁷ It is also established that serine proteases react following the same mechanism.⁸ Recently the complete catalytic cycle of AChE was characterized by QM/MM modeling.⁹ It confirmed that acylation is faster than deacylation and the important role of Glu202 in orienting water molecule for deacylation. Dysfunctions of AChE due to organophosphorus (OP) compounds are a major threat. In fact, OP compounds, used as pesticides and chemical warfare agents, inhibit AChE irreversibly. A covalent bond is formed between the oxygen of Ser203 and the phosphorus of the OP compound (see Scheme 2). It is commonly accepted that the leaving group is *anti* to the oxygen of Ser203.¹⁰ This inhibition by chemical warfare agents can lead to convulsions, for instance, and possibly death by asphyxiation. There-

fore understanding more precisely the mechanism of inhibition of AChE by OP compounds is crucial for the design of reactivation agents, effective in the treatment of OP poisoning. Indeed some theoretical studies dealing with interaction between AChE and the OP compound like sarin have already been performed by Leszczynski et al.¹¹ In particular, in 2008, they used density functional theory (DFT) to look at AChE phosphorylation by sarin on a model system.¹² They showed that the mechanism proceeds via an addition–elimination pathway.

The first step in building a theoretical model for reactivation of OP-AChE is to understand at the molecular level how the OP compound can interact with the catalytic site of AChE. Tabun reactivity is particularly interesting as it is one of the more potent nerve agents, and tabun-inhibited AChE is one of the more difficult complexes to reactivate.^{13–15} Indeed VX-inhibited AChE can be reactivated by oxime HI-6, which is not the case for tabun, for example.¹⁶ Also, tabun is produced as a mixture of two enantiomers, and one of them (the levorotatory isomer, not attributed to a specific enantiomer) is 6.3 times more potent.¹⁷ Could it be that the kinetics are different for the two enantiomers, or is it a different binding mechanism? To outline this question, we studied tabun inhibition of AChE by using a computational approach. More precisely we examined the four possibilities of tabun fixation: the fixation of the (*S*) tabun enantiomer with the cyano group *anti* or *syn* to the oxygen atom of Ser203 (S-Syn and S-Anti); the (*R*) tabun enantiomer with the cyano group *anti* or *syn* to the oxygen atom of Ser203 (R-Syn and R-Anti).

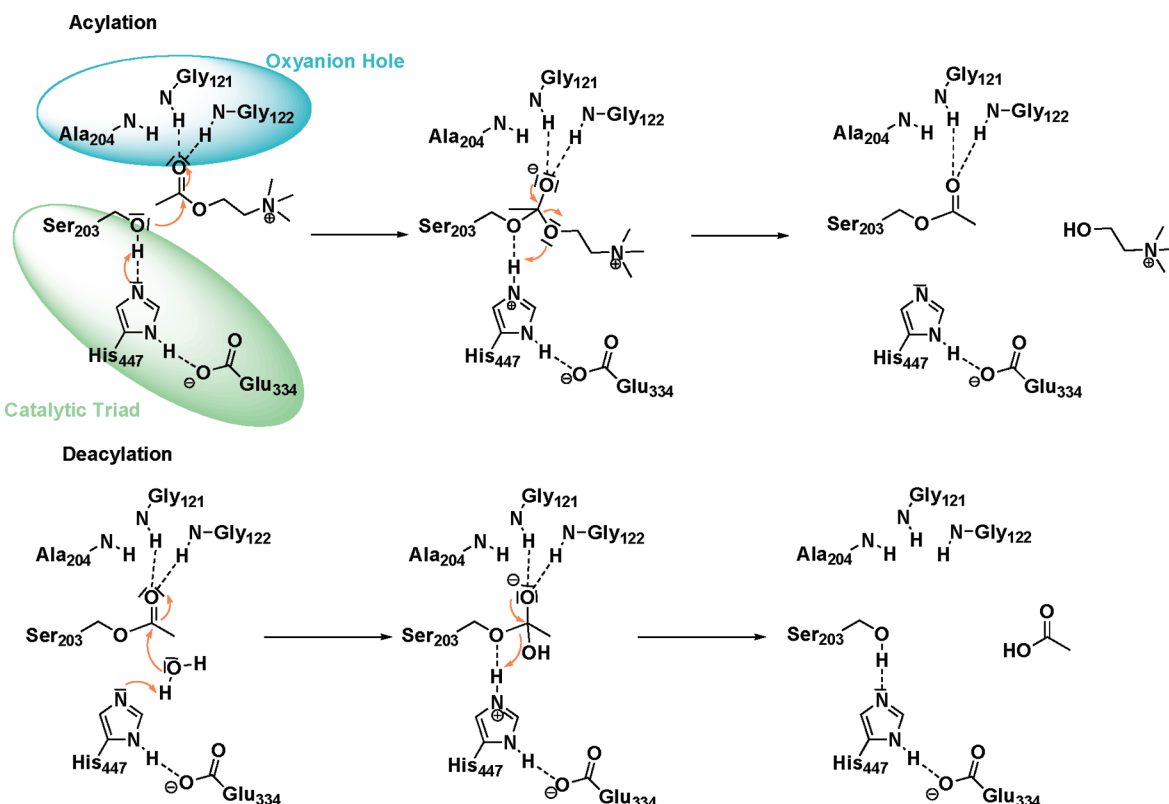
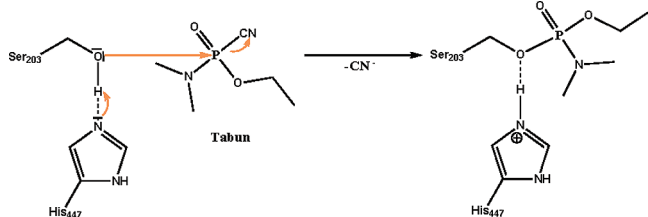
Methods

We addressed this problem by using a QM/MM methodology,¹⁸ which is a method of choice to solve mechanistic issues in enzymes.^{19–22} The QM/MM calculations were carried out with

* Corresponding author. E-mail: etienne.derat@upmc.fr. Tel: +33 1 44 27 59 96. Fax: +33 1 44 27 73 60.

[†] UPMC Univ Paris 06.

[‡] Centre d'Etudes du Bouchet.

SCHEME 1: Mechanism of Hydrolysis of Acetylcholine in Choline and Acetic Acid**SCHEME 2: Irreversible Inhibition of AChE by Tabun**

Chemshell,²³ which interfaces Turbomole²⁴ for the QM subsystem and the CHARMM force field²⁵ using DL_POLY for the MM region. The QM subsystem was carried out with the BP86 functional^{26–28} within the framework of the RI approximation and a triple- ζ basis set (TZVP)²⁹ for geometry optimization. Taking into consideration the system size, BP86 functional is a good compromise between accuracy and calculation time. Single point energy corrections were also performed with the B3LYP^{30–33} or, following Nemukhin's choice,⁹ PBE0 functional³⁴ to check the quality of BP86 results. The starting structure was taken from the Protein Data Bank (PDB). Tabun inhibited AChE has been characterized by Ekström et al.³⁵ Starting from the X-ray data of the aged form of tabun inhibited AChE obtained by Ekström (PDB code 2COP), we have slightly modified the coordinates to add the missing atoms (namely, the *N*-dimethyl group of tabun). The experimental data were obtained for the structure of the complex AChE-tabun after the cyano group has moved out of the active site. We have thus added the cyano group in the two possible configurations with respect to the positions of the *N*-dimethyl group and the ethoxy group of the tabun in the active site. Then the cyano group of the (*R*) tabun enantiomer is *anti* to the oxygen atom of Ser203 (*R*-Anti, called **RA** on the energy profile), which is not the case for the (*S*) tabun enantiomer (*S*-Syn, called **SS** on the energy profile). As seen in Figure 1, the QM subsystem consists of 85

atoms for the first calculations using PDB 2COP (QM part 1). It is composed of tabun and parts of residues Gly121, Gly122, Ser203, Ala204, Ser229, Gly230, Val330, Val331, Glu334, and His447. The active MM region consists of 324 atoms and is composed of residues and water molecules close to the active site: Gly120, Gly121, Gly122, Phe123, Tyr124, Ser125, Glu202, Ser203, Ala204, Ser229, Gly230, Trp236, Phe295, Phe297, Val330, Val331, Glu334, Phe338, Val407, His447, Wat21, Wat99, Wat141, and Wat258. The rest of the enzyme was

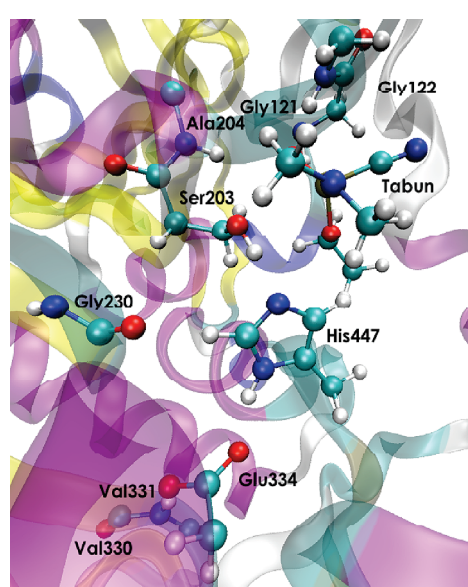


Figure 1. View of the active site of AChE in ball and stick form are shown the residues of the QM subsystem. The snapshot corresponds to **1RA** (*R*-Anti). Ser203, His447, and Glu334 constitute the catalytic triad. The oxyanion hole is composed of Gly121, and Gly122.

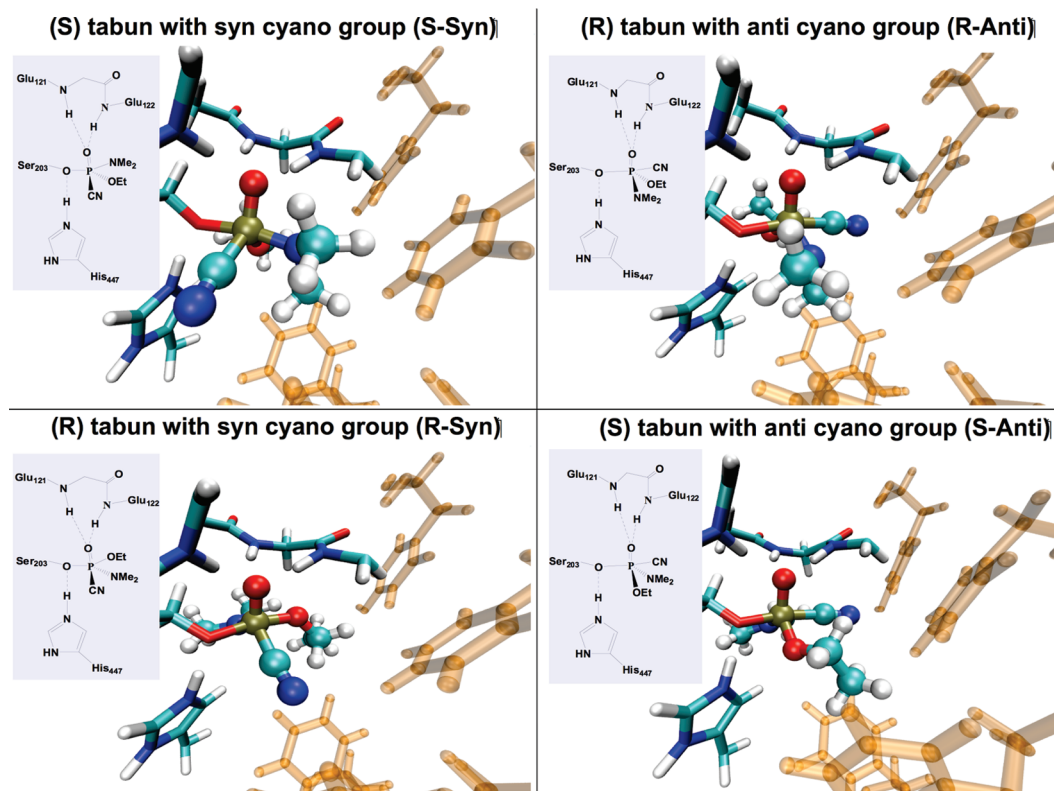


Figure 2. View of the active site of AChE for the four intermediates before the cyano group departure. Ser203, His447, and the oxyanion hole are represented in opaque stick, tabun in ball and sticks, and aromatic residues (Tyr124, Phe295, Phe297, Phe338) in transparent orange stick (PDB 3DL7).

treated as a nonactive MM region; it was taken into account for the calculation of MM energy but was fixed during optimizations. The connections between intermediates and products and between intermediates and reactants were verified by running extensive geometry scans between the critical points. In these scans one degree of freedom was used as a reaction coordinate, while all other degrees of freedom were fully optimized.

We thus obtained the energy profile for the fixation of the two tabun enantiomers which gave the experimental product. Meanwhile, Nacher et al. corrected the PDB 2COP in 2008, and it appeared that aging goes through *O*-dealkylation and not *N*-demethylation.³⁶ This new structure is encoded in the Protein Data Bank as 3DL7. To check whether the two crystallographic structures give the same energy profiles and then whether our results obtained with PDB 2COP are correct or not, we reproduced our calculations with the starting conformation of PDB 3DL7. We used a better QM subsystem for the next calculations with PDB 2COP and PDB 3DL7 than in the first calculations; in particular we paid much attention in the amide function between Gly120 and Gly121. We also cut the residues 229 and 230 of the QM subsystem, because they did not seem to have a role in this reaction according to our previous results. The new QM subsystem consists of 88 atoms (QM part 2). It is composed of tabun and parts of residues Gly120, Gly121, Gly122, Glu202, Ser203, Ala204, Val330, Val331, Glu334, and His447. Calculations with this new QM subsystem used the same functional and basis set as the previous system. We also focused on the kinetically determinant step, which is the cyano group departure. We thus obtained R-Anti and S-Syn profiles with PDB 2COP and 3DL7. With the more recent starting structure (PDB 3DL7), we also explored the two other possibilities of tabun fixation in the active site, that is, the fixation

of the (S) tabun enantiomer with the cyano group *anti* to the oxygen atom of the Ser203 (S-Anti, called SA on the energy profile), and the (R) tabun enantiomer with the cyano group *syn* to the oxygen atom of the Ser203 (R-Syn, called RS on the energy profile). These two possibilities gave a product which has opposite relative positions of the *N*-dimethyl group and the ethoxy group in the active site as compared to the experimental X-ray structure. We have then a complete pattern of reactivity.

Results and Discussion

Figure 2 illustrates the four intermediates (S-Syn, R-Anti, R-Syn, S-Anti) with tabun fixed on the serine oxygen before the cyano group departure. We first studied the energy profiles of R-Anti and S-Syn obtained with the PDB 2COP. The results are represented in Figure 3.

Let us now discuss the energetic pattern for R-Anti and S-Syn. The first step is the addition of tabun phosphorus on the oxygen of Ser203. For R-Anti, a small transition state (**TS12RA**) corresponds to the binding of tabun inside the oxyanion hole; the cost for this reorganization is rather small. A second transition state (**TS23RA**) allows the phosphorus atom to be in close interaction with the serine oxygen. During this step, the proton of Ser203 is transferred to His447. Overall, this binding is energetically favorable by approximately 8 kcal/mol. For S-Syn, a first transition state (**TS12SS**) corresponds to both the binding of tabun close to the oxygen atom of Ser203 and inside the oxyanion hole and the transfer of the proton of Ser203 to His447. The barrier is quite small and the process energetically favorable by approximately 3.5 kcal/mol. It is thus clear that the step of tabun fixation before the cyano group departure is almost barrierless for the two enantiomers.

The second step for the two enantiomers is the cyano group elimination. For the R-Anti cyano group departure (**3RA** →

BP86/TZVP
B3LYP/TZVP//BP86/TZVP
PBE0/TZVP//BP86/TZVP

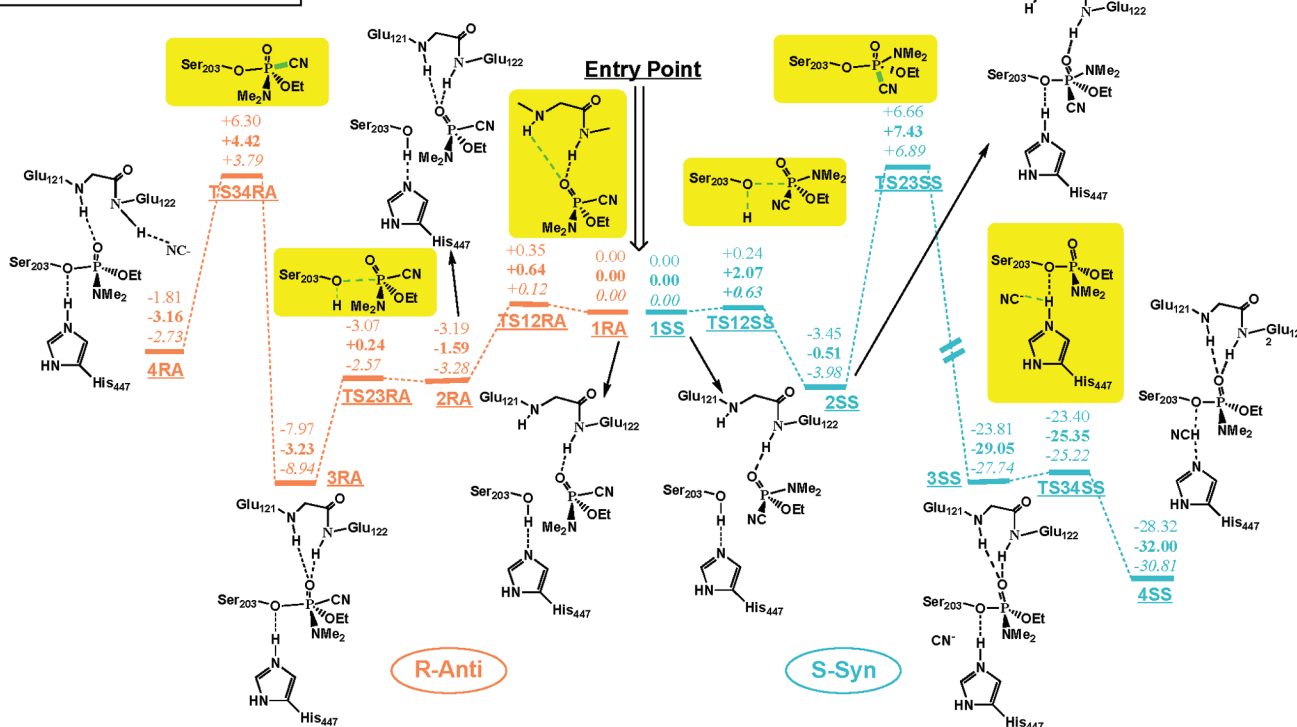


Figure 3. Energy profile for the fixation of the two tabun enantiomers leading to the experimental structure (PDB 2C0P), using BP86/TZVP (non-bold characters), B3LYP/TZVP//BP86/TZVP (bold character), and PBE0/TZVP//BP86/TZVP (italic characters). Data are in kcal/mol.

BP86/TZVP
PBE0/TZVP//BP86/TZVP

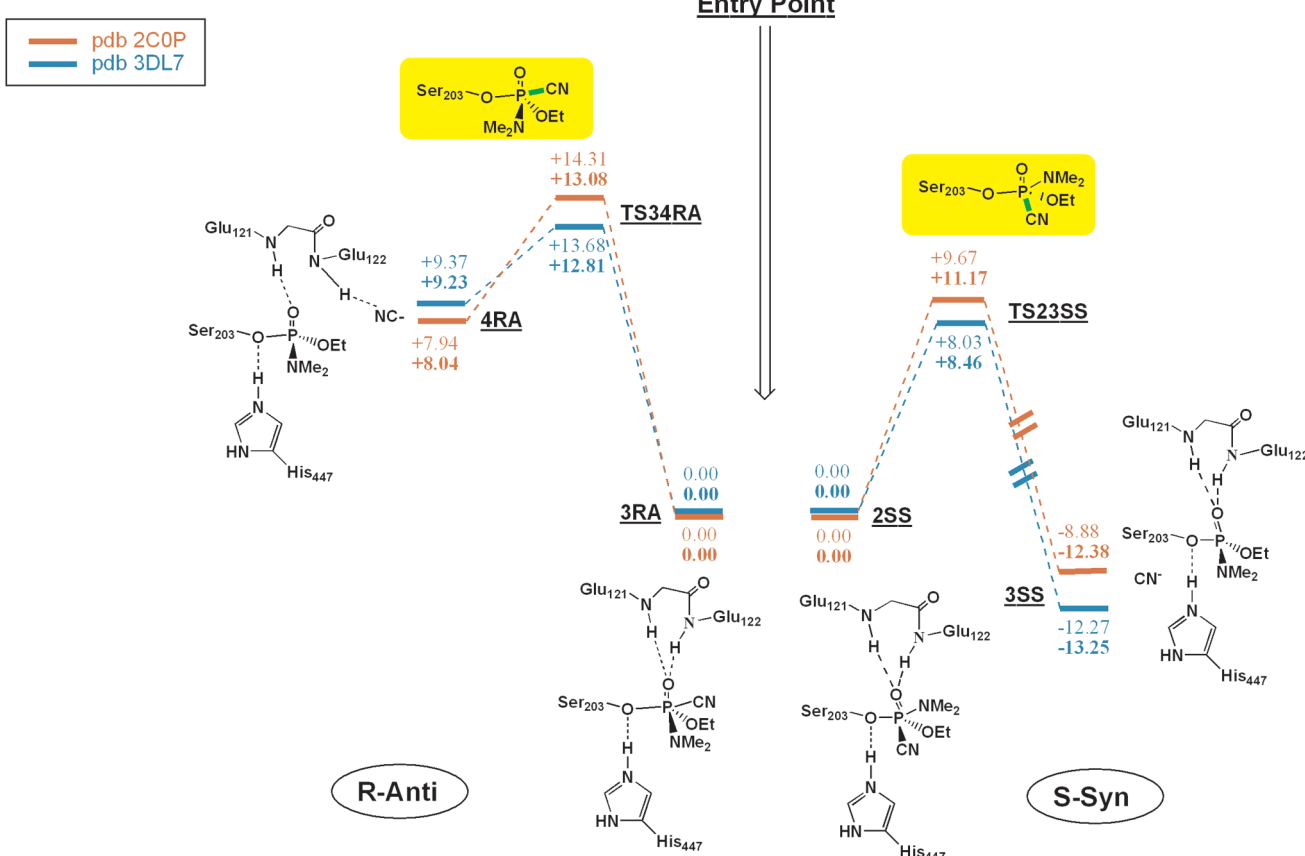


Figure 4. Comparison of energy profile for cyano group departure for PDB 2C0P and PDB 3DL7, using BP86/TZVP (non-bold characters) and PBE0/TZVP//BP86/TZVP (bold characters). Data are in kcal/mol.

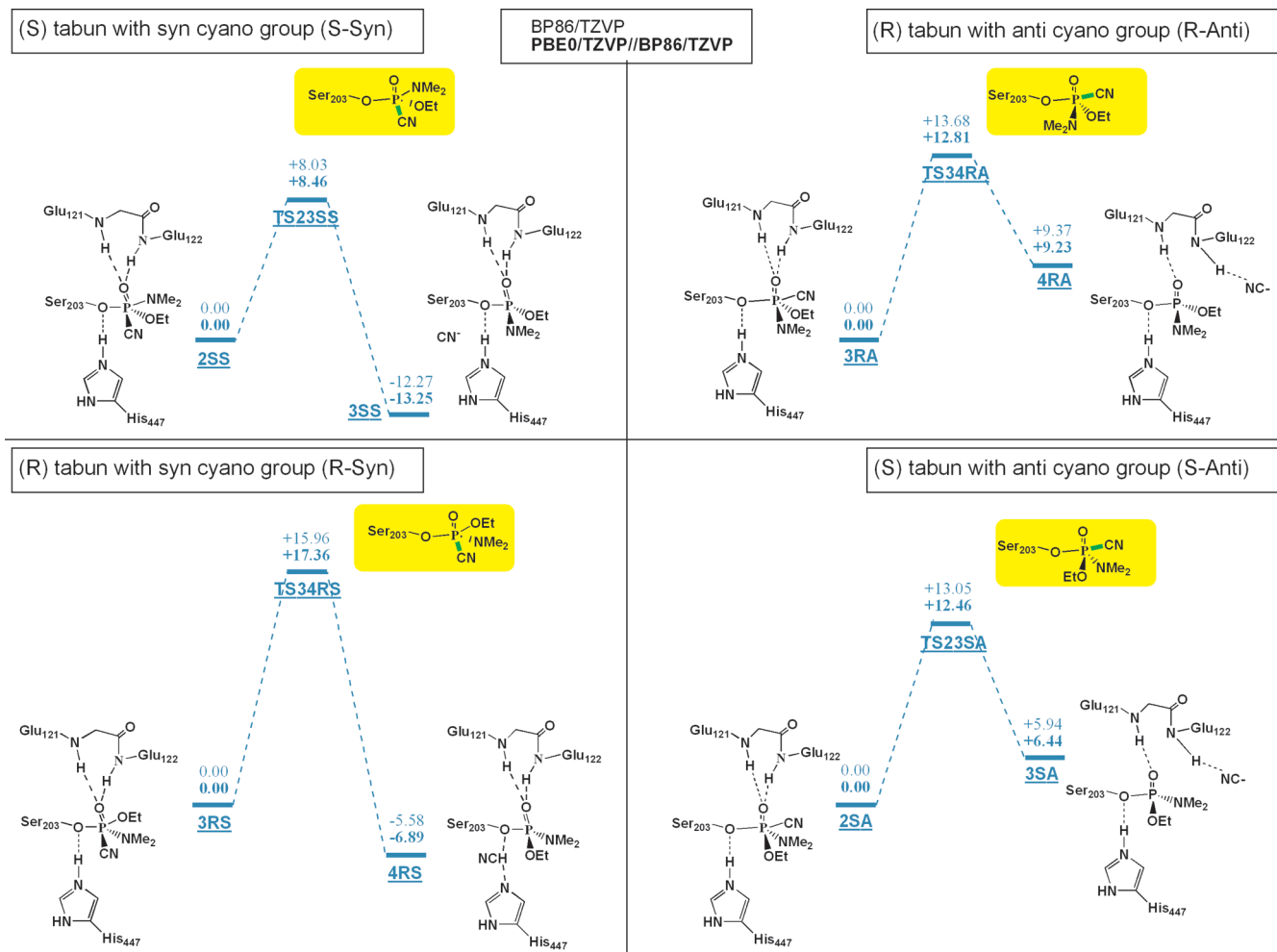


Figure 5. Energy profiles for cyano group departure (PDB 3DL7), using BP86/TZVP (non-bold characters) and PBE0/TZVP//BP86/TZVP (bold characters). Data are in kcal/mol.

TS34RA → 4RA), the barrier is about 14 kcal/mol. It is thus the rate-limiting step for this enantiomer. The product 4RA obtained is not stable according to our QM/MM calculations. Inspection of the structure shows the cyano group is leaving in the direction of a hydrophobic pocket (often called the acyl pocket) containing in particular the residues Phe295, Phe297, and Phe338. Therefore repulsive interactions between the leaving group and the enzyme active site may explain the reaction's endothermic character. For S-Syn, the cyano group departure occurs through TS23SS. At the BP86 level, the barrier is lower than the corresponding one for R-Anti (10.52 vs 14.27 kcal/mol). It is also the rate-limiting step for this enantiomer. What is interesting is the fact that the process is exothermic by roughly 20 kcal/mol, which is not the case for R-Anti, which implies S-Syn is favored. The last transition state for S-Syn (TS34SS) is only a reorganization of the cyano group to create HCN by capturing the proton between Ser203 and His447.

A few differences exist in the geometry of intermediates of R-Anti and S-Syn. The starting structure 1RA has a longer P–O_{Ser203} bond than 1SS (3.02 Å vs 2.48 Å). The P–CN bond length is about 1.80 Å for the two enantiomers. After the addition of the tabun on the Ser203, P–CN bond in 3RA is longer than in 1RA (1.93 Å vs 1.83 Å), and the P–O_{Ser203} bond length in 3RA is 1.80 Å. The P–O_{Ser203} bond grows stronger with the cyano group departure as its length is 1.68 Å in 4RA. The same phenomenon is observed for S-Syn: P–CN bond in 2SS is longer than in 1SS (1.88 Å vs 1.81 Å) but shorter than

the P–CN bond of 3RA (1.88 Å vs 1.93 Å), and the P–O_{Ser203} bond grows stronger with the cyano group departure as its length is 1.61 Å in 3SS.

In these calculations, the two enantiomers leading to the experimental product react via two distinct mechanisms. It seems that the more potent enantiomer is S-Syn contrary to the common idea because of (i) the instability of the product resulting from R-Anti and (ii) the lower energetic barrier of the rate limiting step. To assert these results, the two other possibilities of attack, which do not lead to the experimental structure, should be modeled.

To verify that the two PDB structures give the same energy profiles, the approach of the two tabun enantiomers leading to the experimental structure were modeled with PDB 3DL7 and 2COP. We choose to focus on the cyano group departure since it is the rate-limiting step. For these calculations, we used the QM part 2 previously described. In comparing the energy profiles for these two enantiomers as seen in Figure 4, it appears that there is no significant energetic difference between the two crystallographic structures: S-Syn has an activation energy of 8.03 kcal/mol with PDB 3DL7 and of 9.67 kcal/mol with PDB 2COP. The reaction is exothermic with both structures. The P–O and P–CN bond lengths are comparable between the two PDB for S-Syn (for instance: P–O_{2SS}(2COP) = 1.81 Å, P–CN_{2SS}(2COP) = 1.87 Å vs P–O_{2SS}(3DL7) = 1.80 Å, P–CN_{2SS}(3DL7) = 1.88 Å). As for R-Anti, the activation energy is 13.68 kcal/mol with PDB 3DL7 and 14.31 kcal/mol with PDB

2COP. The reaction is endothermic with the two crystallographic structures. The P–O and P–CN bond lengths are comparable between the two PDB for R-Anti (for instance: P–O_{3RA}(2COP) = 1.84 Å, P–CN_{3RA}(2COP) = 1.92 Å vs P–O_{3RA}(3DL7) = 1.81 Å, P–CN_{3RA}(3DL7) = 1.93 Å). From these data we assert that our results obtained with PDB 2COP are robust enough in considering the starting 3D conformations of the enzyme–inhibitor complex. Because PDB 3DL7 is a corrected version of PDB 2COP, we did the calculations that follow with PDB 3DL7.

These calculations consist of modeling the four possible attacks of the tabun on the oxygen of Ser203: S-Syn and R-Anti which led to experimental X-ray structure and R-Syn and S-Anti leading to a different isomer than was experimentally seen. Figure 5 illustrates the energy profiles obtained for the four cases studied.

The first observation is that regardless of the tabun enantiomer, when the cyano group is *anti* to the oxygen of Ser203, the reaction is not thermodynamically favored. For R-Anti, the reaction is endothermic by about 9 kcal/mol, and for S-Anti, by 6 kcal/mol. Indeed the cyano group is leaving in a hydrophobic pocket as seen before for R-Anti with PDB 2COP. Moreover, the energetic barrier is about 13 kcal/mol for the two enantiomers in this case. In the alternative attack, with the cyano group *syn* to the oxygen of Ser203, the reaction is energetically favorable. It is exothermic by 6 kcal/mol for R-Syn and by 12 kcal/mol for S-Syn. It should be noted, however, that the activation energy is about 8 kcal/mol for S-Syn, while it is almost 17 kcal/mol for R-Syn. Geometry differences between the *syn* and *anti* enantiomers are found in the P–CN and P–O_{Ser203} bonds. The P–CN bond is longer for the *anti* enantiomers (1.93 Å for R-Anti and S-Anti) than for the *syn* enantiomers (1.88 Å for the S-Syn, 1.84 Å for the R-Syn), and the P–O_{Ser203} bond gets shorter during this step in all cases (from around 1.80 Å to 1.65 Å).

It appears that the most favored reaction is the attack of S-Syn. Indeed it corresponds to the exothermic reaction with the lowest energetic barrier. If the (*S*) tabun is considered to be the most active enantiomer, our result (S-Syn is favored) is in total agreement with the experimental data since it gives the X-ray structure. For the (*R*) tabun enantiomer, the favored attack is the one with the cyano group *anti* to the oxygen of Ser203, as it has an energetic barrier of about 14 kcal/mol compared to 17 kcal/mol for R-Syn. Therefore, it is also in agreement with the experimental data (if the (*R*) tabun is considered to be the most active enantiomer). Our results suggest that the enantiomer which is 6.3 times more potent is (*S*) tabun.

Conclusion

We studied the tabun fixation inside the AChE active site. Using the PDB 2COP,³⁵ we examined the fixation of the two enantiomers leading to the experimental X-ray structure, namely, S-Syn and R-Anti. The mechanism goes through an addition–elimination pathway. The kinetically determinant step is the cyano group departure, as tabun fixation on Ser203 departure is almost barrierless.

The PDB 2COP was corrected by Nachon et al. and replaced by the PDB 3DL7.³⁶ The two X-ray structures (PDB 2COP and 3DL7) gave analogous results for the calculations previously described. We then considered the kinetically determinant step with this new PDB. We studied the four possible attacks of tabun on the oxygen of Ser203: S-Syn and R-Anti, which led to the experimental X-ray structure, and S-Anti and R-Syn, which led to the isomer which has opposite relative positions

of the *N*-dimethyl group and the ethoxy group in the active site as compared to the experimental structure. It appears that the most active enantiomer is S-Syn. Thus it seems that the cyano group does not leave *anti* to the oxygen of Ser203, as expected, due to repulsive polar interaction between cyanide and aromatic residues in the active site, in particular Phe295, Phe297, and Phe338. This QM/MM study is a first step in understanding the interaction between AChE and tabun in a theoretical way. The same study is currently underway for sarin since the most active enantiomer is identified and the complex AChE-sarin has been crystallized.³⁷ The next step is to consider organophosphorus inhibited AChE reactivation by oximes to clarify how reactivation works and then design more efficient oximes.

Acknowledgment. We thank UPMC, CNRS, and IUF. O.K. thanks DGA for Ph.D. funding. This work was supported by ANR BLAN06-2_159258 and BLAN0309 “Radicauxverts”.

Supporting Information Available: Energetics and QM Cartesian coordinates for all the calculated species. This material is available free of charge via the Internet at <http://pubs.acs.org>.

References and Notes

- (1) Soreq, H.; Seidman, S. *Nat. Rev.: Neuroscience* **2001**, 2, 295.
- (2) (a) Quinn, D. M. *Chem. Rev.* **1987**, 87, 955. (b) Silman, I.; Sussman, J. L. *Chem.-Biol. Interact.* **2008**, 175, 3.
- (3) Colletier, J.-P.; Fournier, P.; Greenblatt, H. M.; Stojan, J.; Sussman, J. L.; Zaccai, G.; Silman, I.; Weik, M. *EMBO J.* **2006**, 25, 2746.
- (4) Sussman, J. L.; Harel, M.; Frolow, F.; Oefner, C.; Goldman, A.; Toker, L.; Silman, I. *Science* **1991**, 253, 872.
- (5) Bourne, Y.; Radić, Z.; Sulzenbacher, G.; Kim, E.; Taylor, P.; Marchot, P. *J. Biol. Chem.* **2006**, 281, 29256.
- (6) (a) Warshel, A.; Naray-Szabo, G.; Sussman, F.; Hwang, J. K. *Biochemistry* **1989**, 28, 3629. (b) Fuxreiter, M.; Warshel, A. *J. Am. Chem. Soc.* **1998**, 120, 183.
- (7) Zhang, Y.; Kua, J.; McCammon, J. A. *J. Am. Chem. Soc.* **2002**, 124, 10572.
- (8) Ishida, T.; Kato, S. *J. Am. Chem. Soc.* **2003**, 125, 12035.
- (9) Nemukhin, A. V.; Lushchekina, S. V.; Bochenkova, A. V.; Golubeva, A. A.; Varfolomeev, S. D. *J. Mol. Model.* **2008**, 14, 409.
- (10) (a) Millard, C. B.; Kryger, G.; Ordentlich, A.; Greenblatt, H. M.; Harel, M.; Raves, M. L.; Segall, Y.; Barak, D.; Shafferman, A.; Silman, I.; Sussman, J. L. *Biochemistry* **1999**, 38, 7032. (b) Ordentlich, A.; Barak, D.; Kronman, C.; Ariel, N.; Segall, Y.; Velan, B.; Shafferman, A. *J. Biol. Chem.* **1996**, 271, 11953.
- (11) (a) Majumdar, D.; Roszak, S.; Leszczynski, J. *J. Phys. Chem. B* **2006**, 110, 13597. (b) Paukku, Y.; Michalkova, A.; Majumdar, D.; Leszczynski, J. *Chem. Phys. Lett.* **2006**, 422, 317.
- (12) Wang, J.; Gu, J.; Leszczynski, J. *J. Phys. Chem. B* **2008**, 112, 3485.
- (13) Kuca, K.; Kassa, J. *Enzyme Inhib. Med. Chem.* **2003**, 18, 529.
- (14) Cabal, J.; Kuca, K.; Kassa, J. *Basic & Clinical Pharmacology & Toxicology* **2004**, 95, 81.
- (15) Kuca, K.; Jun, D.; Cabal, J.; Musilova, L. *Basic Clin. Pharmacol. Toxicol.* **2007**, 101, 25.
- (16) (a) Worek, F.; Widmann, R.; Knopff, O.; Szinicz, L. *Arch. Toxicol.* **1998**, 72, 237. (b) Worek, F.; Thiermann, H.; Szinicz, L.; Eyer, P. *Biochem. Pharmacol.* **2004**, 68, 2237.
- (17) Degenhardt, C.; Van Der Berg, G. R.; De Jong, L. P. A.; Benschop, H. P. *J. Am. Chem. Soc.* **1986**, 108, 8290.
- (18) For a small selection of reviews, see: (a) Aqvist, J.; Warshel, A. *Chem. Rev.* **1993**, 93, 2523. (b) Gao, J. In *Reviews in Computational Chemistry*; Lipkowitz, K. B., Boyd, D. B., Eds.; VCH: Weinheim, 1995; Vol. 7, p 119. (c) Mordini, T. Z.; Thiel, W. *Chimia* **1998**, 52, 288. (d) Monard, G.; Merz, K. M., Jr. *Acc. Chem. Res.* **1999**, 32, 904. (e) Sherwood, P. In *Modern Methods and Algorithms of Quantum Chemistry*; Grotenhorst, J., Ed.; NIC Series 3; John von Neumann Institute for Computing: Jülich, 2000 p 285. (f) Gao, J.; Truhlar, D. G. *Annu. Rev. Phys. Chem.* **2002**, 53, 467–505. (g) Field, M. J. *J. Comput. Chem.* **2002**, 23, 48. (h) Monard, G.; Prat-Rosina, X.; Gonzalez-Lafont, A.; LLuch, J. M. *Int. J. Quantum Chem.* **2003**, 93, 229. (i) Ridder, L.; Mulholland, A. *Curr. Top. Med. Chem.* **2003**, 3, 1241.
- (19) Derat, E.; Shaik, S. *J. Am. Chem. Soc.* **2006**, 128, 13940.
- (20) Cho, K.-B.; Derat, E.; Shaik, S. *J. Am. Chem. Soc.* **2007**, 129, 3182.
- (21) Chen, H.; Moreau, Y.; Derat, E.; Shaik, S. *J. Am. Chem. Soc.* **2008**, 130, 1953.

- (22) Cho, K.-B.; Hirao, H.; Chen, H.; Carvajal, M. A.; Cohen, S.; Derat, E.; Thiel, W.; Shaik, S. *J. Phys. Chem. A* **2008**, *112*, 13128.
- (23) Sherwood, P.; de Vries, A. H.; Guest, M. F.; Schreckenbach, G.; Catlow, C. R. A.; French, S. A.; Sokol, A. A.; Bromley, S. T.; Thiel, W.; Turner, A. J.; Billeter, S.; Terstegen, F.; Thiel, S.; Kendrick, J.; Rogers, S. C.; Casci, J.; Watson, M.; King, F.; Karlsen, E.; Sjøvoll, M.; Fahmi, A.; Schäfer, A.; Lennartz, C. *J. Mol. Struct. (THEOCHEM)* **2003**, *632*, 1.
- (24) Ahlrichs, R.; Bär, M.; Häser, M.; Horn, H.; Kölmel, C. *Chem. Phys. Lett.* **1989**, *162*, 165.
- (25) MacKerell, A. D., Jr.; Bashford, D.; Bellott, M.; Dunbrack, R. L., Jr.; Evanseck, J. D.; Field, M. J.; Fischer, S.; Gao, J.; Guo, H.; Ha, S.; Joseph-McCarthy, D.; Kuchnir, L.; Kuczera, K.; Lau, F. T. K.; Mattos, C.; Michnick, S.; Ngo, T.; Nguyen, D. T.; Prodhom, B.; Reiher, W. E., III; Roux, B.; Schlenkrich, M.; Smith, J. C.; Stote, R.; Straub, J.; Watanabe, M.; Wiorkiewicz-Kuczera, J.; Yin, D.; Karplus, M. *J. Phys. Chem. B* **1998**, *102*, 3586.
- (26) Vosko, S.; Wilk, L.; Nusair, M. *Can. J. Phys.* **1980**, *58*, 1200.
- (27) Becke, A. D. *Phys. Rev. A* **1988**, *38*, 3098.
- (28) Perdew, J. P. *Phys. Rev. B* **1986**, *33*, 8822.
- (29) Schäfer, A.; Huber, C.; Ahlrichs, R. *J. Chem. Phys.* **1994**, *100*, 5829.
- (30) Becke, A. D. *Phys. Rev. A* **1988**, *38*, 3098.
- (31) Becke, A. D. *J. Chem. Phys.* **1993**, *98*, 1372.
- (32) Becke, A. D. *J. Chem. Phys.* **1993**, *98*, 5648.
- (33) Lee, C.; Yang, W.; Parr, R. G. *Phys. Rev. B* **1988**, *37*, 785.
- (34) Adamo, C.; Barone, V. *J. Chem. Phys.* **1999**, *110*, 6158.
- (35) Ekström, F.; Akfur, C.; Tunemalm, A.-K.; Lundberg, S. *Biochemistry* **2006**, *45*, 74.
- (36) Carletti, E.; Li, H.; Li, B.; Ekström, F.; Nicolet, Y.; Loiodice, M.; Gillon, E.; Froment, M. T.; Lockridge, O.; Schopfer, L. M.; Masson, P.; Nachon, F. *J. Am. Chem. Soc.* **2008**, *130*, 16011.
- (37) (a) Benschop, H. P.; De Jong, L. P. A. *Acc. Chem. Res.* **1988**, *21*, 368. (b) Li, W.; Lum, K. T.; Chen-Goodspeed, M.; Sogorb, M. A.; Raushel, F. M. *Bioorg. Med. Chem.* **2001**, *9*, 2083.

JP903843S